Published by
NIGERIAN SOCIETY OF PHYSICAL SCIENCES
Available online @ https://journal.nsps.org.ng/index.php/jnsps

J. Nig. Soc. Phys. Sci. 6 (2024) 2052

Journal of the Nigerian Society of Physical Sciences

Throughflow effect on bi-disperse convection in Rivlin-Ericksen fluid

Pushap Lata Sharma[a], Deepak Bains[a], Pankaj Thakur[b,*]

[a]Department of Mathematics & Statistics, Himachal Pradesh University, Summer Hill, Shimla, 171005, India
[b]Faculty of Science and Technology, ICFAI University, Baddi, Solan, 180004, India

Abstract

In this investigation, we delve into the influence of throughflow on the phenomenon of bi-disperse convection within Rivlin-Ericksen fluid. In the context of examining bi-disperse convection within this specific type of fluid, the throughflow effect is considered to have a uniform vertical distribution. The primary focus of this study centers on evaluating the system's linear stability. To achieve this, we employ normal mode analysis to compute the Darcy-Rayleigh number at the onset of convection. This Darcy-Rayleigh number is computed for both stationary and oscillatory convection modes. Furthermore, we conduct a comprehensive analysis and present the results in graphical form to illustrate the impact of various parameters, including Peclet number and kinematic viscoelastic parameter, on both stationary and oscillatory convection. Our research findings demonstrate that when Peclet number $\mathrm{Pr}_1 < 0$, it leads to destabilising effect on both stationary and oscillatory convections. Conversely, when Peclet number $\mathrm{Pr}_1 > 0$, it induces stabilising effect on both stationary as well as oscillatory convections.

DOI:10.46481/jnsps.2024.2052

Keywords: Bi-disperse porous medium, Normal mode analysis, Rivlin-Ericksen fluid, Throughflow effect

Article History :
Received: 27 March 2024
Received in revised form: 20 May 2024
Accepted for publication: 22 May 2024
Published: 04 June 2024

Communicated by: Babatunde James Falaye

1. Introduction

Bi-disperse convection refers to the examination of convective flow initiation within materials possessing dual porosity characteristics, which are denoted as bi-disperse porous media. These bi-disperse porous materials, or bi-disperse porous media (BDPM), exhibit distinctive features in the form of two distinct types of pores: macropores and micropores. More specifically, the macropores are identified as the f-phase, representing the fractured phase, while the remaining structural components are designated as the p-phase, signifying the porous phase. Bi-disperse porous media find applications in various fields, including heat pipe evaporators, culinary processes, solar thermal systems, permafrost studies, heat exchangers, computer systems, electronics, nuclear energy conversion, assessment of effective thermal conductivity in sintered porous materials, water filtration using filter tubes, capillary structures, the exploration of subsurface drinking water supply physics, chemistry, chemical engineering, chromatography, coal storage, gas shale storage, hydraulic fracturing of underground rock formations for natural gas extraction and the investigation of landslide phenomena. Chen *et al.* [1] have contributed to this field by conducting both theoretical and experimental studies focused on the characterization of the stagnant thermal conductivity of

*Corresponding author: Tel.: +918570975865
Email address: pankaj@journal.nsps.org.ng (Pankaj Thakur)

bi-disperse porous media.

Nield and Kuznetsov [2–4] in their contributions, advanced a sophisticated mathematical model that explains the initiation of bi-disperse convection. Their analysis covered the derivation of analytical solutions for fully developed forced convection within a bi-dispersed porous medium. Furthermore, in the case of fully developed convection, their investigation yielded expressions that establish the Nusselt number as a function of the inherent properties of the bi-disperse porous medium (BDPM). Nield and Kuznetsov [4] proved that the $(R_D)_{cri}$ for the onset of bi-disperse convection is higher with respect to $(R_D)_{cri}$ for the single porosity case. Therefore dual-porosity materials are better materials in solving insulation problems and thermal management problems. Consequently, bi-disperse porous materials provide much more materials possibilities to design man-made materials for heat transfer problems. For this reason, recently, the onset of bi-disperse convection has become an interesting topic to investigate for many researchers such as Imani *et al.* [5], Gentile and Straughan [6], Gentile *et al.* [7], Badday *et al.* [8], Falsaperla *et al.* [9] and Capone *et al.* [10].

Rivlin-Ericksen fluid, a type of non-Newtonian fluid, is characterized by its ability to exhibit both viscous and elastic behaviour under flow. This unique rheological property makes it suitable for various industrial applications, including polymer processing, biomedicine and material science. In polymer processing, it is utilized in the manufacturing of products like films, fibers and coatings due to its shear-thinning behaviour. In biomedicine, it finds application in drug delivery systems and tissue engineering for its tunable viscosity and visco-elastic properties. Furthermore, in material science, Rivlin-Ericksen fluids are studied for their role in understanding complex flow phenomena and designing advanced materials with tailored mechanical properties. Several researchers, including Rana and Thakur [11], Chand and Rana [12, 13], Rana [14] and Rana *et al.* [15, 16], have dedicated their research efforts to investigating the properties and behavior of Rivlin-Ericksen fluid.

"Throughflow" typically denotes the movement or transport of a substance, such as water or air, through a medium or material, such as soil or a porous substance. This terminology is commonly employed within the areas of hydrology and soil science. Throughflow represents a critical element of the hydrological cycle, governing the flow of water within earth's ecosystems. It holds significant ecological and environmental ramifications as it facilitates the transportation of nutrients, pollutants and sediments across the landscape. The comprehension of throughflow is of paramount importance in water resource management, enabling an assessment of the influence of land use and land management practices on water quality and availability. The horizontal subsurface movement of water, known as throughflow, typically occurs when the soil reaches a state of complete saturation and it exerts a significant influence on convective instabilities. When a net vertical mass flow (throughflow) occurs across a horizontally heated layer from below, the stability of this motion becomes a fundamental concern. This is especially relevant in applications encompassing cloud physics, astrophysics, hydrological and geophysical investigations, seabed hydrodynamics, subterranean pollution studies and various industrial and technological processes. The investigation of convection in throughflow has attracted attention from multiple researchers, including Sutton [17], Petrolo *et al.* [18] and Capone *et al.* [19, 20]. Notably, Capone *et al.* [20] investigated the impact of throughflow on bi-disperse convection, with a particular focus on single-temperature bi-disperse porous media. Their study based on the utilization of weighted energy method to capture the most suitable description of the underlying physics in this context. Further, there are several authors: Ruo *et al.* [21], Reddy and Ragoju [22] and Awasthi *et al.* [23] who have considered throughflow effect in their respective researches.

Chandrasekhar [24], in his book, conducted all stability analyses using normal mode analysis. Normal mode analysis plays a crucial role in understanding thermal instability by quantifying the growth or decay rates of perturbations and determining the dominant modes that lead to instability. This approach is widely employed in physics, engineering and other scientific disciplines to study the stability and dynamics of systems ranging from mechanical vibrations to electromagnetic waves. Recently, the researchers like: Sharma *et al.* [25, 26], Bains *et al.* [27], Sharma *et al.* [28, 29] and Bains *et al.* [30] have analysed their investigations in different aspects by making use of normal mode analysis.

In this scientific inquiry, we have undertaken a thorough examination, considering the practical applications and the substantial importance of bi-disperse porous media (BDPM) in addressing complex thermal management challenges. Additionally, we recognize the relevance of managing and controlling convective instabilities in the broader context of thermal and engineering sciences. Our investigation is focused on a comprehensive exploration of the impact of throughflow on bi-disperse convection, with a specific emphasis on its manifestation within a viscoelastic fluid, where we have selected the Rivlin-Ericksen fluid as our model system. The analysis of this study is conducted using the normal mode approach, encompassing both stationary and oscillatory modes, to provide a comprehensive understanding of the phenomena under investigation.

2. Mathematical formulation and governing the equations

Here, we investigate thermal instability of throughflow effect on bi-disperse porous medium (BDPM) that is saturated with Rivlin-Ericksen fluid. This BDPM is positioned within a spatial domain defined by the planes $z = 0$ and $z = d$. It undergoes uniform heating from its lower boundary, influenced by the gravitational field represented as $\mathbf{g} = (0, 0, -g)$. The variables T_L and T_U represent the temperatures at the lower plane $z = 0$ and the upper plane $z = d$, respectively, with the condition that $T_L > T_U$. Additionally, we make the assumption that the BDPM exhibits a single-temperature characteristic, signifying that temperatures T^p and T^f within the medium are equivalent and designated as T (see Figure 1).

Now, utilizing the Boussinesq approximation, which aligns with the principles of entropy, we can establish the governing equations based on Darcy's model, as per the work of Capone

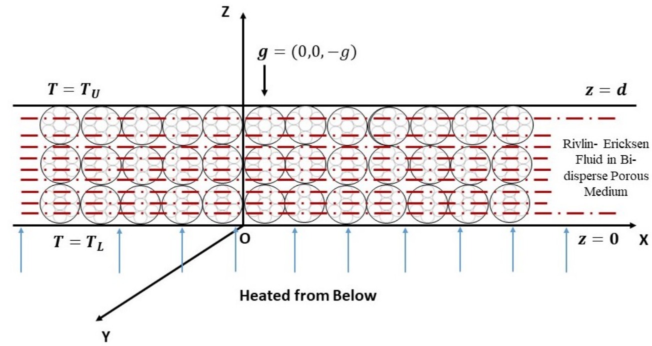

Figure 1. Physical Configuration.

et al. [20]:

$$\nabla.\mathbf{q}^f = 0, \tag{1}$$

$$\nabla.\mathbf{q}^P = 0, \tag{2}$$

$$-\frac{1}{K_f}\left(\mu + \mu'\frac{\partial}{\partial t}\right)\mathbf{q}^f - \zeta\left(\mathbf{q}^f - \mathbf{q}^P\right) - \nabla p^f - \rho_0\alpha\mathbf{g}T = 0, \tag{3}$$

$$-\frac{1}{K_P}\left(\mu + \mu'\frac{\partial}{\partial t}\right)\mathbf{q}^P - \zeta\left(\mathbf{q}^P - \mathbf{q}^f\right) - \nabla p^P - \rho_0\alpha\mathbf{g}T = 0, \tag{4}$$

$$(\rho c)_m\frac{\partial T}{\partial t} + (\rho c)_f\left(\mathbf{q}^P + \mathbf{q}^f\right).\nabla T = k_m\nabla^2 T, \tag{5}$$

where $\mathbf{q}^S$ and p^S are seepage velocity and pressure field for $S = \{f, P\}$, respectively, T is temperature, μ is viscosity of the fluid, μ' is visco-elasticity of the fluid, ζ denotes interaction coefficient between the $f-$phase and $p-$phase, K_S denotes permeabilities for $S = \{f, P\}$, k_m is thermal conductivity (following Capone *et al.* [20]).

$$(\rho c)_m = (1-\varphi)(1-\varepsilon)(\rho c)_{sol} + \varphi(\rho c)_f + \varepsilon(1-\varphi)(\rho c)_P,$$
$$k_m = (1-\varphi)(1-\varepsilon)k_{sol} + \varphi k_f + \varepsilon(1-\varphi)k_P,$$

where subscript *sol* referred to solid skeleton.

Given that we are restricting our analysis to a scenario involving a single-temperature bi-disperse porous medium, with both macropores and micropores being saturated by the same fluid, we anticipate that $(\rho c)_f$ and $(\rho c)_P$ will be equivalent [9, 20], hence

$$(\rho c)_m = (1-\varphi)(1-\varepsilon)(\rho c)_{sol} + [\varphi + \varepsilon(1-\varphi)](\rho c)_f.$$

Our objective is to conduct a stability analysis of a vertical throughflow occurring within the layer. Consequently, we can establish the boundary conditions as [20]:

$$\left.\begin{array}{l}\mathbf{q}^P = \left(0,0,Q^P\right),\ \ \mathbf{q}^f = \left(0,0,Q^f\right),\ \ T = T_L \ \text{ at } z = 0\\ \mathbf{q}^P = \left(0,0,Q^P\right),\ \ \mathbf{q}^f = \left(0,0,Q^f\right),\ \ T = T_U \ \text{ at } z = d\end{array}\right\}. \tag{6}$$

3. Basic state solutions

The assumed basic state is:

$$\left.\begin{array}{l}\mathbf{q}^f = \left(0,0,q^f\right),\quad \mathbf{q}^P = \left(0,0,q^P\right),\\ T = T_b(z),\quad p^P = p_b^P(z),\quad p^f = p_b^f(z)\end{array}\right\}. \tag{7}$$

Utilizing equation (7) within the preceding equations (1)-(5), we have

$$\frac{dq^f}{dz} = 0, \tag{8}$$

$$\frac{dq^P}{dz} = 0, \tag{9}$$

$$-\frac{1}{K_f}\left(\mu + \mu'\frac{\partial}{\partial t}\right)\mathbf{q}^f - \zeta\left(\mathbf{q}^f - \mathbf{q}^P\right) - \frac{d}{dz}\left(p_b^f(z)\right) - \rho_0\alpha\mathbf{g}T_b(z) = 0, \tag{10}$$

$$-\frac{1}{K_P}\left(\mu + \mu'\frac{\partial}{\partial t}\right)\mathbf{q}^P - \zeta\left(\mathbf{q}^P - \mathbf{q}^f\right) - \frac{d}{dz}\left(p_b^P(z)\right) - \rho_0\alpha\mathbf{g}T_b(z) = 0, \tag{11}$$

$$(\rho c)_f\left(\mathbf{q}^P + \mathbf{q}^f\right)\frac{d}{dz}\left(T_b(z)\right) = k_m\frac{d^2}{dz^2}\left(T_b(z)\right). \tag{12}$$

Subsequently incorporating the boundary condition given in (6) into the preceding equations (8) and (9), we arrive at:

$$\mathbf{q}^f = Q^f\hat{k} \quad \text{and} \quad \mathbf{q}^P = Q^P\hat{k}, \tag{13}$$

additionally, by applying boundary condition in equation (6) to equation (12), we have

$$T_b(z) = \frac{T_U - T_L e^{\frac{\bar{Q}d(\rho c)_f}{k_m}} + (T_L - T_U)e^{\frac{\bar{Q}z(\rho c)_f}{k_m}}}{1 - e^{\frac{\bar{Q}d(\rho c)_f}{k_m}}}, \tag{14}$$

where $\bar{Q} = Q^f + Q^P$.

Hence, the solutions for the steady state of Rivlin-Ericksen fluid with vertical throughflow are expressed as:

$$\mathbf{q}^f = Q^f\hat{k},\ \mathbf{q}^P = Q^P\hat{k},$$
$$T_b(z) = \frac{T_U - T_L e^{\frac{\bar{Q}d}{\kappa_m}} + (T_L - T_U)e^{\frac{\bar{Q}z}{\kappa_m}}}{1 - e^{\frac{\bar{Q}d}{\kappa_m}}}. \tag{15}$$

The outcome expressed in equation (15) corresponds exactly to the results reported by Capone *et al.* [20].

4. Perturbation solutions

For the stability analysis, we have incorporated minor disturbances into the basic state as:

$$\left.\begin{array}{l}\mathbf{q}^f = \left(0,0,q^f\right) + \mathbf{q}'^f = \left(0,0,q^f\right) + \left(u'^f, v'^f, w'^f\right),\\ \mathbf{q}^P = \left(0,0,q^P\right) + \mathbf{q}'^P = \left(0,0,q^P\right) + \left(u'^P, v'^P, w'^P\right),\\ T = T_b + T',\quad p^P = p_b^P + \pi'^P,\quad p^f = p_b^f + \pi'^f.\end{array}\right\} \tag{16}$$

Now, incorporating equation (16) into equations (1) – (6) and omitting the prime notation (′) for the sake of convenience, we have:

$$\nabla.\mathbf{q}^f = 0, \tag{17}$$

$$\nabla.\mathbf{q}^P = 0, \tag{18}$$

$$-\frac{1}{K_f}\left(\mu + \mu'\frac{\partial}{\partial t}\right)\mathbf{q}^f - \zeta\left(\mathbf{q}^f - \mathbf{q}^P\right) - \nabla\pi^f + \rho_0\alpha g T\hat{k} = 0, \tag{19}$$

$$-\frac{1}{K_P}\left(\mu + \mu'\frac{\partial}{\partial t}\right)\mathbf{q}^P - \zeta\left(\mathbf{q}^P - \mathbf{q}^f\right) - \nabla\pi^P + \rho_0\alpha g T\hat{k} = 0, \tag{20}$$

$$(\rho c)_m\frac{\partial T}{\partial t} + \frac{(\rho c)_f\left(w^f + w^P\right)(T_L - T_U)}{1 - e^{\frac{\bar{Q}d}{\kappa_m}}}\left(\frac{\bar{Q}}{\kappa_m}\right)e^{\frac{\bar{Q}z}{\kappa_m}} + (\rho c)_f\bar{Q}\frac{\partial T}{\partial z} = k_m\nabla^2 T, \tag{21}$$

and perturbed boundary conditions are

$$w^P = w^f = T = 0 \quad \text{at} \quad z = 0 \quad \text{and} \quad z = d. \tag{22}$$

Furthermore, we have defined dimensionless variables in the following manner [6, 20]:

$$\left.\begin{array}{c} (x^*, y^*, z^*) = \frac{(x,y,z)}{d}, \quad t^* = \frac{tk_m}{(\rho c)_m d^2}, \\ \mathbf{q}^{P*} = \frac{\mathbf{q}^P d}{\kappa_m}, \quad \mathbf{q}^{f*} = \frac{\mathbf{q}^f d}{\kappa_m}, \\ \pi^{f*} = \frac{\pi^f}{\kappa_m\zeta}, \quad \pi^{P*} = \frac{\pi^P}{\kappa_m\zeta}, \quad T^* = \frac{T}{\sqrt{\frac{\beta\kappa_m\zeta}{\rho_0\alpha g}}} \end{array}\right\}. \tag{23}$$

Applying equation (23) to the previously outlined equations (17) – (22) and removing the star symbol (∗) for ease of representation, we obtain the simplified dimensionless equations as follows:

$$\nabla.\mathbf{q}^f = 0, \tag{24}$$

$$\nabla.\mathbf{q}^P = 0, \tag{25}$$

$$-\psi_1\left(1 + F\frac{\partial}{\partial t}\right)\mathbf{q}^f - \left(\mathbf{q}^f - \mathbf{q}^P\right) - \nabla\pi^f + \sqrt{R_D}T\hat{k} = 0, \tag{26}$$

$$-\psi_2\left(1 + F\frac{\partial}{\partial t}\right)\mathbf{q}^P - \left(\mathbf{q}^P - \mathbf{q}^f\right) - \nabla\pi^P + \sqrt{R_D}T\hat{k} = 0, \tag{27}$$

$$\frac{\partial T}{\partial t} + \mathrm{Pr}_1\frac{\partial T}{\partial z} + L_1\sqrt{R_D}\left(w^f + w^P\right) = \nabla^2 T, \tag{28}$$

and the dimensionless boundary conditions are

$$w^P = w^f = T = 0 \quad \text{at} \quad z = 0 \quad \text{and} \quad z = 1, \tag{29}$$

where the dimensionless parameters are [6, 20]:
Kinematic visco-elastic parameter $F = \frac{\mu' k_m}{\mu(\rho c)_m d^2}$, $\psi_1 = \frac{\mu}{\zeta K_f}$, $\psi_2 = \frac{\mu}{\zeta K_P}$, Peclet number $\mathrm{Pr}_1 = \frac{\bar{Q}d}{\kappa_m}$, Darcy-Rayleigh number $R_D = \left(\frac{\rho_0\alpha g\beta d^2}{\zeta\kappa_m}\right)^{\frac{1}{2}}$ and dimensionless basic temperature gradient $L_1 = \frac{\mathrm{Pr}_1 e^{\mathrm{Pr}_1 z}}{1 - e^{\mathrm{Pr}_1}}$.

Now operating equations (26) and (27) by $\hat{k}.curl.curl$, we get

$$\psi_1\left(1 + F\frac{\partial}{\partial t}\right)\nabla^2 w^f + \nabla^2\left(w^f - w^P\right) - \sqrt{R_D}\nabla_H^2 T = 0, \tag{30}$$

$$\psi_2\left(1 + F\frac{\partial}{\partial t}\right)\nabla^2 w^P + \nabla^2\left(w^P - w^f\right) - \sqrt{R_D}\nabla_H^2 T = 0. \tag{31}$$

5. Normal mode analysis and dispersion relation

The examination of the system's stability is conducted by utilizing the normal mode technique, in accordance with the approach presented by Chandrasekhar [24]:

$$\left[w^f, w^P, T\right] = \left[W(z), \Phi(z), \Theta(z)\right]\exp\left(ixk_x + iyk_y + nt\right). \tag{32}$$

By incorporating equation (32) in above equations (28) – (31), we have

$$\psi_1(1 + nF)\left(D^2 - a^2\right)W + \left(D^2 - a^2\right)[W - \Phi] + \sqrt{R_D}a^2\Theta = 0, \tag{33}$$

$$\psi_2(1 + nF)\left(D^2 - a^2\right)\Phi + \left(D^2 - a^2\right)[\Phi - W] + \sqrt{R_D}a^2\Theta = 0, \tag{34}$$

$$n\Theta + \mathrm{Pr}_1 D\Theta + \frac{\mathrm{Pr}_1\sqrt{R_D}e^{\mathrm{Pr}_1 z}}{1 - e^{\mathrm{Pr}_1}}[W + \Phi] = \left(D^2 - a^2\right)\Theta. \tag{35}$$

Furthermore, the boundary conditions are simplified to the form outlined by Chandrasekhar [24] when applying the normal mode analysis:

$$W = D^2W = \Phi = D^2\Phi = \Theta = 0 \ \text{at} \ z = 0 \ \text{and} \ z = 1, \tag{36}$$

where, $D = \frac{d}{dz}$, $-a^2 = \nabla_H^2 = \frac{\partial^2}{\partial x^2} + \frac{\partial^2}{\partial y^2}$ and $\nabla^2 = D^2 - a^2$.

Consider the trial solutions for W, Φ, Θ of the form following Chandrasekhar [24]:

$$W = W_0 \sin(\pi z), \ \Phi = \Phi_0 \sin(\pi z), \ \Theta = \Theta_0 \sin(\pi z). \tag{37}$$

The solutions presented in equation (37) comply with the boundary conditions as delineated in equation (36).

Substituting (37) into equations (33) – (35) and performing integration for each equation over the range of $z = 0$ and $z = 1$, we obtain:

$$\begin{bmatrix} J[1 + \psi_1(1 + nF)] & -J & -a^2\sqrt{R_D} \\ -J & J[1 + \psi_2(1 + nF)] & -a^2\sqrt{R_D} \\ \frac{\pi^2\mathrm{Pr}_1\sqrt{R_D}(1 + e^{\mathrm{Pr}_1})}{(1 - e^{\mathrm{Pr}_1})(\pi^2 + \mathrm{Pr}_1^2)} & \frac{\pi^2\mathrm{Pr}_1\sqrt{R_D}(1 + e^{\mathrm{Pr}_1})}{(1 - e^{\mathrm{Pr}_1})(\pi^2 + \mathrm{Pr}_1^2)} & 2(J + n) \end{bmatrix}\begin{bmatrix} W_0 \\ \Theta_0 \\ \Phi_0 \end{bmatrix} = \begin{bmatrix} 0 \\ 0 \\ 0 \end{bmatrix}. \tag{38}$$

The presence of non-trivial solution within the linear system (38) occurs if and only if

$$R_D = \frac{2J\,(J+n)\left(1-e^{\mathrm{Pr}_1}\right)\left(\pi^2+\mathrm{Pr}_1^2\right)\{1-[1+A_1]\,[1+A_2]\}}{a^2\pi^2\mathrm{Pr}_1\,(1+e^{\mathrm{Pr}_1})\,\{4+A_1+A_2\}}, \tag{39}$$

where $A_1 = \psi_1\,(1+nF)$, $A_2 = \psi_2\,(1+nF)$ and $J = \pi^2 + a^2$.

5.1. Stationary convection

In the context of stationary convection, by putting $n = 0$ in equation (39), we get:

$$(R_D)_{sta} = \frac{2J^2\left(1-e^{\mathrm{Pr}_1}\right)\left(\pi^2+\mathrm{Pr}_1^2\right)\{1-(1+\psi_1)\,(1+\psi_2)\}}{a^2\pi^2\mathrm{Pr}_1\,(1+e^{\mathrm{Pr}_1})\,(4+\psi_1+\psi_2)}. \tag{40}$$

The critical value of Darcy-Rayleigh number of above equation (40) exists at $a_{cri} = \pi$.

6. Oscillatory convection

For oscillatory convection put $n = in_i$ in equation (39), we have

$$R_D = \frac{2J\,(J+in_i)\left(1-e^{\mathrm{Pr}_1}\right)\left(\pi^2+\mathrm{Pr}_1^2\right)\{1-[1+A_{11}]\,[1+A_{22}]\}}{a^2\pi^2\mathrm{Pr}_1\,(1+e^{\mathrm{Pr}_1})\,\{4+A_{11}+A_{22}\}}, \tag{41}$$

where, $A_{11} = \psi_1\,(1+in_iF)$, $A_{22} = \psi_2\,(1+in_iF)$.

Now, upon partitioning equation (41) into its real and imaginary constituents, we obtain:

$$R_D = \Delta_1 + in_i\Delta_2, \tag{42}$$

where

$$\Delta_1 = \frac{2J\left(1-e^{\mathrm{Pr}_1}\right)\left(\pi^2+\mathrm{Pr}_1^2\right)(B_1+B_2)}{a^2\pi^2\mathrm{Pr}_1\,(1+e^{\mathrm{Pr}_1})\left\{(4+\psi_1+\psi_2)^2+n_i^2F^2(\psi_1+\psi_2)^2\right\}},$$

and

$$\Delta_2 = \frac{2J\left(1-e^{\mathrm{Pr}_1}\right)\left(\pi^2+\mathrm{Pr}_1^2\right)(B_3-B_4)}{a^2\pi^2\mathrm{Pr}_1\,(1+e^{\mathrm{Pr}_1})\left\{(4+\psi_1+\psi_2)^2+n_i^2F^2(\psi_1+\psi_2)^2\right\}},$$

here,

$$B_1 = (4+\psi_1+\psi_2)\left\{J\left[n_i^2F^2\psi_1\psi_2-(\psi_1+\psi_2+\psi_1\psi_2)\right] + n_i^2F(\psi_1+\psi_2+2\psi_1\psi_2)\right\},$$

$$B_2 = n_i^2F\,(\psi_1+\psi_2)\left\{\left[n_i^2F^2\psi_1\psi_2-(\psi_1+\psi_2+\psi_1\psi_2)\right] - JF(\psi_1+\psi_2+2\psi_1\psi_2)\right\},$$

$$B_3 = (4+\psi_1+\psi_2)\left\{\left[n_i^2F^2\psi_1\psi_2-(\psi_1+\psi_2+\psi_1\psi_2)\right] - JF(\psi_1+\psi_2+2\psi_1\psi_2)\right\},$$

and

$$B_4 = F\,(\psi_1+\psi_2)\left\{J\left[n_i^2F^2\psi_1\psi_2-(\psi_1+\psi_2+\psi_1\psi_2)\right] + n_i^2F(\psi_1+\psi_2+2\psi_1\psi_2)\right\}.$$

With oscillatory onset $\Delta_2 = 0$ and $n_i \neq 0$, we get

$$n_i^2 = \frac{P_1-P_2}{P_3}, \tag{43}$$

where

$$P_1 = (\psi_1+\psi_2+\psi_1\psi_2)\,(4+\psi_1+\psi_2-FJ\,(\psi_1+\psi_2)),$$
$$P_2 = FJ\,(4+\psi_1+\psi_2)\,(\psi_1+\psi_2+2\psi_1\psi_2),$$

and

$$P_3 = F^2\left\{\psi_1\psi_2\Big(4+\psi_1+\psi_2-FJ(\psi_1+\psi_2)\Big) - (\psi_1+\psi_2)(\psi_1+\psi_2+2\psi_1\psi_2)\right\}.$$

Then from equation (42), we have

$$(R_D)_{osc} = \frac{2J\left(1-e^{\mathrm{Pr}_1}\right)\left(\pi^2+\mathrm{Pr}_1^2\right)(B_{11}+B_{22})}{a^2\pi^2\mathrm{Pr}_1\,(1+e^{\mathrm{Pr}_1})\left\{(4+\psi_1+\psi_2)^2+n_i^2F^2(\psi_1+\psi_2)^2\right\}}. \tag{44}$$

where

$$B_{11} = (4+\psi_1+\psi_2)\left\{J\left[n_i^2F^2\psi_1\psi_2-(\psi_1+\psi_2+\psi_1\psi_2)\right] + n_i^2F(\psi_1+\psi_2+2\psi_1\psi_2)\right\},$$

$$B_{22} = n_i^2F\,(\psi_1+\psi_2)\left\{\left[n_i^2F^2\psi_1\psi_2-(\psi_1+\psi_2+\psi_1\psi_2)\right] - JF(\psi_1+\psi_2+2\psi_1\psi_2)\right\},$$

here, n_i^2 is as represented by above equation (43). The expression found in equation (44) serves as the representation of the Darcy-Rayleigh number specifically for oscillatory convection.

7. Results and discussions

In this paper, we have analysed the linear stability of throughflow effect on bi-disperse convection in Rivlin-Ericksen fluid. For the linear stability analysis, we have employed the

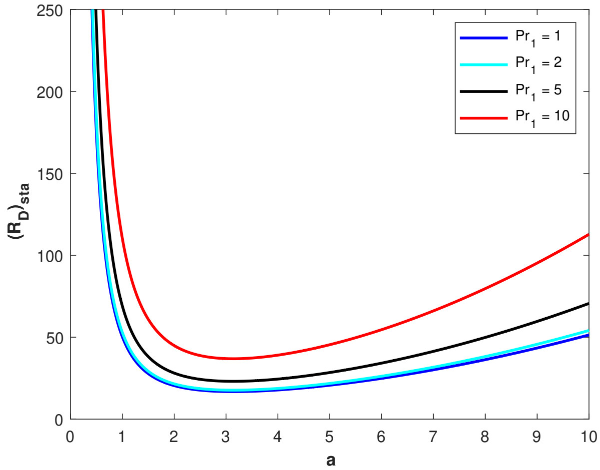

Figure 2. Variation of $(R_D)_{sta}$ w.r.t. a, when $\mathrm{Pr}_1 > 0$.

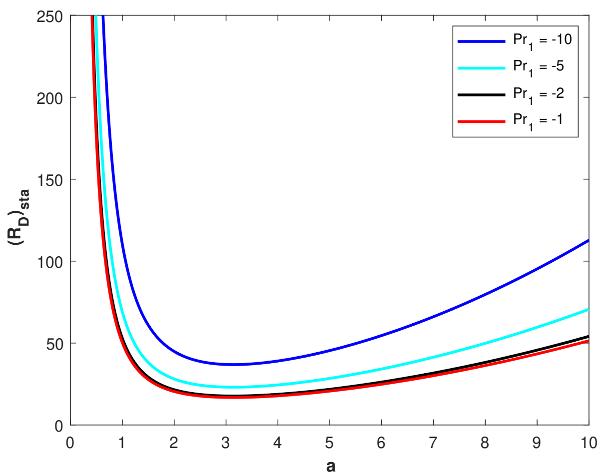

Figure 3. Variation of $(R_D)_{sta}$ w.r.t. a, when $\mathrm{Pr}_1 < 0$.

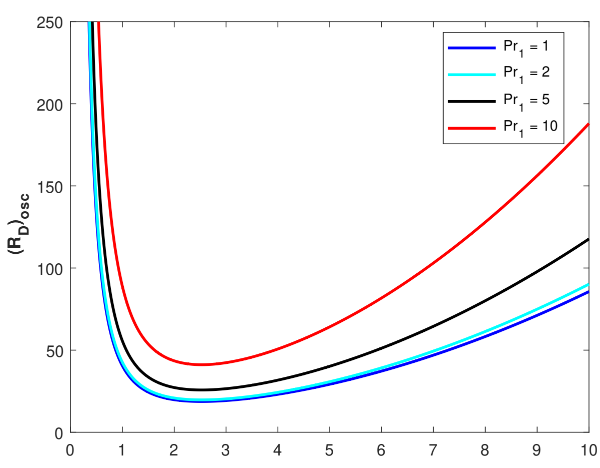

Figure 4. Variation of $(R_D)_{osc}$ w.r.t. a, when $\mathrm{Pr}_1 > 0$.

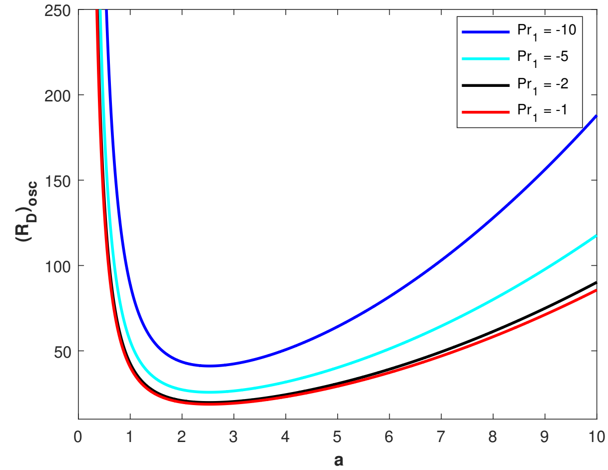

Figure 5. Variation of $(R_D)_{osc}$ w.r.t. a, when $\mathrm{Pr}_1 < 0$.

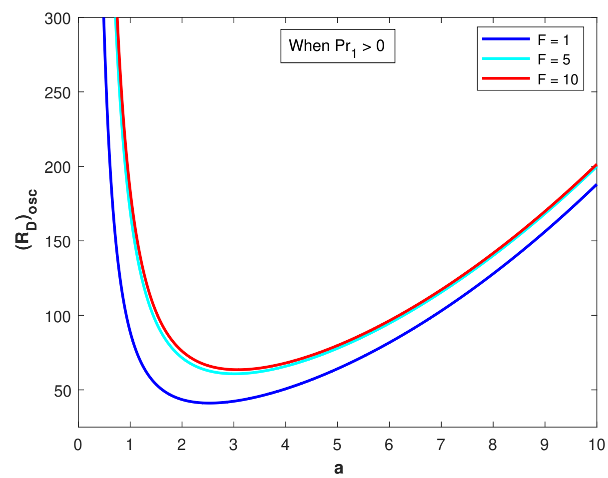

Figure 6. Variation of $(R_D)_{osc}$ w.r.t. a for distinct values of kinematic viscoelastic parameter F, when $\mathrm{Pr}_1 > 0$.

normal mode analysis for both stationary as well as oscillatory convections. The effect of Peclet number has been analysed and presented graphically for both stationary as well as oscillatory convections. Further, we have also analysed the effect of kinematic viscoelastic parameter on oscillatory convection.

Figure 2 represents the relationship between the Darcy-Rayleigh number (R_D) and the wave number (a) in the context of stationary convection, while adhering to the constraint that Peclet number $\mathrm{Pr}_1 > 0$ and holding constant values of ψ_1 at 2 and ψ_2 at 0.2. The observations derived from Figure 2 lead to the inference that, in the presence of $\mathrm{Pr}_1 > 0$, $(R_D)_{sta}$ exhibits a consistent upward trend with an increasing wave number a. Consequently, it can be deduced that the system exerts a stabilising influence on the phenomenon of stationary convection when Pr_1 is greater than zero.

Figure 3 shows a graphical representation of the relationship between the Rayleigh number (R_D) and the wave number (a) within the context of stationary convection, while following

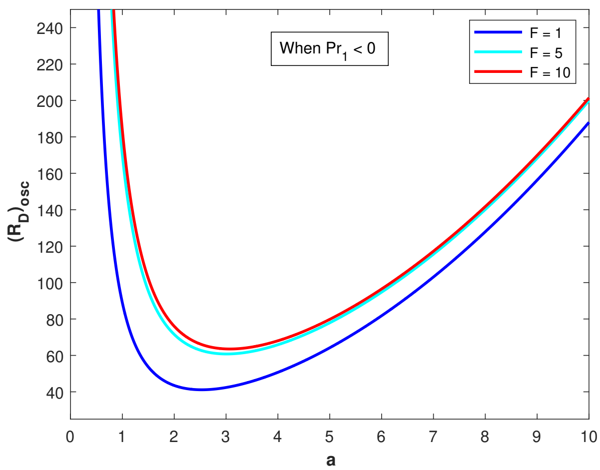

Figure 7. Variation of $(R_D)_{osc}$ w.r.t. a for distinct values of kinematic viscoelastic parameter F, when $\mathrm{Pr}_1 < 0$.

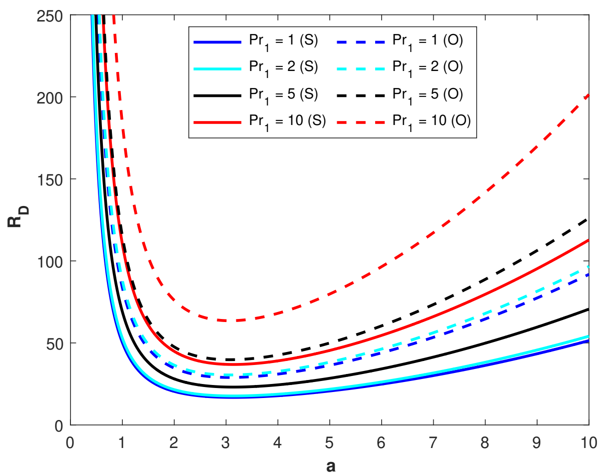

Figure 8. Variation of R_D (for both stationary and oscillatory convection) w.r.t. a, when $\mathrm{Pr}_1 > 0$.

the condition that the Peclet number $\mathrm{Pr}_1 < 0$, with constant values of ψ_1 set at 2 and ψ_2 at 0.2. The analysis of Figure 3 yields the conclusion that, under condition where Pr_1 is less than zero, there is a noticeable decrease in $(R_D)_{sta}$ as the wave number a increases. Consequently, it implies that the system exerts a destabilising influence upon stationary convection when Pr_1 is less than zero.

Figure 4 presents a graphical representation of the dependency of the Darcy-Rayleigh number (R_D) on the wave number (a) in the context of oscillatory convection, while adhering to the condition that Peclet number Pr_1 is greater than zero and holding constant values of ψ_1 at 2 and ψ_2 at 0.2. Analysis of Figure 4 yields the conclusion that, in the presence of Pr_1 greater than zero, $(R_D)_{osc}$ exhibits a positive linear relationship with the wave number a. As a result, it can be inferred that the system exerts a stabilising influence on oscillatory convection under the condition of Pr_1 greater than zero.

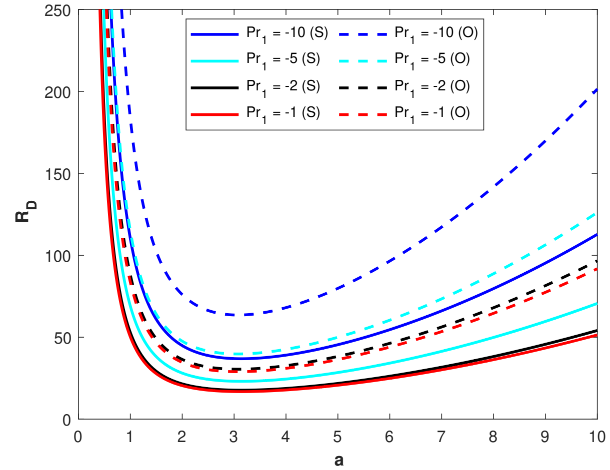

Figure 9. Variation of R_D (for both stationary and oscillatory convection) w.r.t. a, when $\mathrm{Pr}_1 < 0$.

Figure 5 represents the graphical relationship between the Darcy-Rayleigh number (R_D) and the wave number (a) within the framework of oscillatory convection, while maintaining the condition that the Peclet number Pr_1 is less than zero, while keeping ψ_1 fixed at 2 and ψ_2 at 0.2. A thorough examination of Figure 5 leads to the inference that, in scenarios where $\mathrm{Pr}_1 < 0$, there is a consistent decline in $(R_D)_{osc}$ with an increase in the wave number a. As a result, it can be deduced that the system induces a destabilizing influence on oscillatory convection when $\mathrm{Pr}_1 < 0$.

In this research study, the kinematic viscoelastic parameter (F) exhibits its effect exclusively in the domain of oscillatory convection, with no noticeable impact on stationary convection. Figure 6 and Figure 7 provide graphical representations of the impact of the kinematic viscoelastic parameter (F) on oscillatory convection. Figure 6 describes the relationship between the Darcy-Rayleigh number $(R_D)_{osc}$ and the wave number (a) when the Peclet number Pr_1 exceeds zero, while Figure 7 illustrates the same relationship when $\mathrm{Pr}_1 < 0$. Examination of both figures reveals a consistent and positive correlation between $(R_D)_{osc}$ and the wave number a, across various values of $F = 1, 5, 10$. This leads to the inference that the kinematic viscoelastic parameter (F) exerts a stabilising effect on oscillatory convection, regardless of whether Pr_1 is greater than or less than zero.

In Figure 8, we have conducted an analysis that integrates the concurrent effects of both stationary and oscillatory convection, charting the relationship between the Darcy-Rayleigh number (R_D) and the wave number (a) under the condition where the Peclet number Pr_1 exceeds zero. These investigations were carried out while keeping the parameters ψ_1 and ψ_2 fixed at 2 and 0.2, respectively. Figure 8 clearly illustrates that R_D increases with the increase in the wave number a for all values of $\mathrm{Pr}_1 > 0$ and this trend holds true for both stationary as well as oscillatory convections. However, it is important to note that within the realm of oscillatory convection, the system seems to exert a more pronounced stabilising effect when $\mathrm{Pr}_1 > 0$, as compared to the context of stationary convection.

In Figure 9, we conducted an integrated analysis that accounts for the collective influences of both stationary and oscillatory convections. We examined the variation of the Rayleigh number (R_D) with respect to the wave number (a) while keeping the Prandtl number (Pr_1) less than zero and maintaining fixed values of ψ_1 and ψ_2 at 2 and 0.2, respectively. The findings depicted in Figure 9 clearly demonstrate a consistent decrease in R_D as the wave number a increases when $\mathrm{Pr}_1 < 0$, a pattern that is evident in both stationary and oscillatory convections. Interestingly, within the context of stationary convection, the system appears to exhibit a more pronounced destabilising effect when $\mathrm{Pr}_1 < 0$, in contrast to the behaviour observed in oscillatory convection.

8. Conclusions

In this research article, we have analysed the linear stability of throughflow effect on bi-disperse convection in Rivlin-Ericksen fluid. The effect of throughflow is considered as vertically constant in this investigation. This study focuses upon the linear stability of the opted system and here, linear stability analysis is acquired through normal mode analysis. This analysis is carried out for both stationary as well as oscillatory convections. The conclusions are based on the graphical analysis of the opted problem.

We have drawn the following conclusions from the graphs as:

1. The Peclet number Pr_1 exerts a stabilizing influence on both stationary and oscillatory convection patterns when $\mathrm{Pr}_1 > 0$ and the system demonstrates a more pronounced stabilising effect, particularly in the context of oscillatory convection.
2. The Peclet number Pr_1 imparts a destabilizing impact on both stationary and oscillatory convection modes when $\mathrm{Pr}_1 < 0$, with a more accentuated destabilising effect being evident, particularly in the case of stationary convection.
3. The influence of the kinematic viscoelastic parameter (F) is restricted to oscillatory convection and consistently manifests as a stabilising factor, irrespective of whether Pr_1 is less than zero or greater than zero.
4. The study of throughflow effect on bi-disperse convection in Rivlin-Ericksen fluids has broad interdisciplinary implications, ranging from industrial processes to environmental and biomedical applications, offering opportunities for innovation and advancement in multiple fields.

Acknowledgment

The second author expresses appreciation for the financial support provided by UGC for NFSC.

References

[1] Z. Q. Chen, P. Cheng & C. T. Hsu, “A theoretical and experimental study on stagnant thermal conductivity of bi-dispersed porous media”, International Communications in Heat and Mass Transfer **27** (2000) 601. https://doi.org/10.1016/S0735-1933(00)00142-1.

[2] D. A. Nield & A. V. Kuznetsov, “A two-velocity temperature model for a bi-dispersed porous medium: forced convection in a channel”, Transport in Porous Media **59** (2005) 325. https://doi.org/10.1007/s11242-004-1685-y.

[3] D. A. Nield & A. V. Kuznetsov, “Heat transfer in bidisperse porous media”, Transport Phenomena in Porous Media **III** (2005) 34. https://doi.org/10.1016/B978-008044490-1/50006-5.

[4] D. A. Nield & A. V. Kuznetsov, “The onset of convection in a bidisperse porous medium”, International Journal of Heat and Mass Transfer **49** (2006) 3068. https://doi.org/10.1016/j.ijheatmasstransfer.2006.02.008.

[5] G. Imani & K. Hooman, “Lattice Boltzmann pore scale simulation of natural convection in a differentially heated enclosure filled with a detached or attached bidisperse porous medium”, Transport in Porous Media **116** (2017) 91. https://doi.org/10.1007/s11242-016-0766-z.

[6] M. Gentile & B. Straughan, “Bidispersive thermal convection”, International Journal of Heat and Mass Transfer **114** (2017) 837. https://doi.org/10.1016/j.ijheatmasstransfer.2017.06.095.

[7] M. Gentile & B. Straughan, “Bidispersive thermal convection with relatively large macropores”, Journal of Fluid Mechanics **898** (2020) A14. https://doi.org/10.1017/jfm.2020.411.

[8] A. J. Badday & A. J. Harfash, “Chemical reaction effect on convection in bidispersive porous medium”, Transport in Porous Media **137** (2021) 381. https://doi.org/10.1007/s11242-021-01566-6.

[9] P. Falsaperla, G. Mulone & B. Straughan, “Bidispersive-inclined convection”, Proceedings of the Royal Society A: Mathematical, Physical and Engineering Sciences **472** (2016) 20160480. https://doi.org/10.1098/rspa.2016.0480.

[10] F. Capone, R. De Luca, L. Fiorentino & G. Massa, “Bi-disperse convection under the action of an internal heat source”, International Journal of Non-Linear Mechanics **150** (2023) 104360. https://doi.org/10.1016/j.ijnonlinmec.2023.104360.

[11] G. C. Rana & R. C. Thakur, “Effect of suspended particles on thermal convection in Rivlin-Ericksen fluid in a Darcy-Brinkman porous medium”, Journal of Mechanical Engineering and Sciences **2** (2012) 162. https://doi.org/10.15282/jmes.2.2012.3.0014%20.

[12] R. Chand & G. C. Rana, “Dufour and Soret effects on the thermosolutal instability of Rivlin-Ericksen elastico-viscous fluid in porous medium”, Zeitschrift für Naturforschung A **67** (2012) 685. https://doi.org/10.5560/zna.2012-0074.

[13] R. Chand & G. C. Rana, “Thermal instability of Rivlin–Ericksen elastico-viscous nanofluid saturated by a porous medium”, Journal of fluids engineering **134** (2012) 121203. https://doi.org/10.1115/1.4007901.

[14] G. C. Rana, “Hydromagnetic thermosolutal instability of Rivlin-Ericksen rotating fluid permeated with suspended particles and variable gravity field in porous medium”, Acta Universitatis Sapientiae **6** (2014) 24. https://doi.org/10.2478/ausm-2014-0016.

[15] G. C. Rana & R. Chand, “Stability analysis of double-diffusive convection of Rivlin-Ericksen elastico-viscous nanofluid saturating a porous medium: a revised model”, Forschung im Ingenieurwesen **79** (2015) 87. https://doi.org/10.1007/s10010-015-0190-5.

[16] G. C. Rana, R. Chand & V. Sharma, “Thermal instability of a Rivlin-Ericksen nanofluid saturated by a Darcy-Brinkman porous medium: a more realistic model”, Engineering Transactions **64** (2016) 271. https://doi.org/10.24423/engtrans.368.2016.

[17] F. M. Sutton, “Onset of convection in a porous channel with net through flow”, Physics of Fluids **13** (1970) 1931. https://doi.org/10.1063/1.1693188.

[18] D. Petrolo, L. Chiapponi, S. Longo, M. Celli, A. Barletta & V. Di Federico, “Onset of Darcy-Bénard convection under throughflow of a shear-thinning fluid”, Journal of Fluid Mechanics **889** (2020) R2. https://doi.org/10.1017/jfm.2020.84.

[19] F. Capone, J. A. Gianfrani, G. Massa & D. A. S. Rees, “ A weakly nonlinear analysis of the effect of vertical throughflow on Darcy- Bénard convection”, Physics of Fluids **35** (2023) 014107. https://doi.org/10.1063/5.0135258.

[20] F. Capone, R. De Luca, & G. Massa, "Throughflow effect on bi-disperse convection", Ricerche di Matematica **73** (2024) 67. https://doi.org/10.1007/s11587-023-00811-y.

[21] A. C. Ruo, W. M. Yan & M. H. Chang, "The onset of natural convection in a horizontal nanofluid layer heated from below", Heat Transfer **50** (2021) 7764. https://doi.org/10.1002/htj.22252.

[22] G. S. Reddy & R. Ragoju, "Thermal instability of a power-law fluid-saturated porous layer with an internal heat source and vertical through-flow", Heat Transfer **51** (2022) 2181. https://doi.org/10.1002/htj.22395.

[23] M.K. Awasthi, N. Dutt, A. Kumar & S. Kumar, "Electrohydrodynamic capillary instability of Rivlin–Ericksen viscoelastic fluid film with mass and heat transfer", Heat Transfer **53** (2023) 115. https://doi.org/10.1002/htj.22944.

[24] S. Chandrasekhar, *Hydrodynamic and hydromagnetic stability*, Dover Publications, Inc., New York, 2013. https://www.amazon.com/Hydrodynamic-Hydromagnetic-Stability-International-Monographs/dp/048664071X.

[25] P. L. Sharma, D. Bains & P. Thakur, "Thermal instability of rotating Jeffrey nanofluids in porous media with variable gravity", Journal of the Nigerian Society of Physical Sciences **5** (2023) 1366. https://doi.org/10.46481/jnsps.2023.1366.

[26] P. L. Sharma, D. Bains & G. C. Rana, "Effect of variable gravity on thermal convection in Jeffrey nanofluid: Darcy-Brinkman Model", Numerical Heat Transfer, Part B: Fundamentals **85** (2023) 776. https://doi.org/10.1080/10407790.2023.2256970.

[27] D. Bains & P. L. Sharma, "Thermal instability of hydro-magnetic Jeffrey nanofluids in porous media with variable gravity for: free-free, rigid-rigid and rigid-free boundaries", Special Topics & Reviews in Porous Media: An International Journal **15** (2024) 51. https://doi.org/10.1615/SpecialTopicsRevPorousMedia.2023048444.

[28] P. L. Sharma, D. Bains, A. Kumar & P. Thakur, "Effect of rotation on thermosolutal convection in Jeffrey nanofluid with porous medium", Structural Integrity and Life **23** (2023) 299. http://divk.inovacionicentar.rs/ivk/ivk23/299-IVK3-2023-PLS-DB-AK-PT.pdf.

[29] P. L. Sharma, D. Bains & G. C. Rana, "On thermal convection in rotating Casson nanofluid permeated with suspended particles in a Darcy-Brinkman porous medium", Journal of Porous Media **27** (2024) 73. https://doi.org/10.1615/JPorMedia.2024052821.

[30] D. Bains & P. L. Sharma, "Effect of variable gravity on thermal convection in rotating Jeffrey nanofluid: Darcy-Brinkman model", Special Topics & Reviews in Porous Media: An International Journal **15** (2024) 25. https://doi.org/10.1615/SpecialTopicsRevPorousMedia.2023049875.